

Energy spectra of secondaries in proton-proton interactions

S. Koldobskiy^{1,2}, M. Kachelrieß³, A. Lskavyan¹, A. Neronov^{4,5}, S. Ostapchenko^{6,7}, and D. V. Semikoz^{1,4,8}

¹*National Research Nuclear University MEPhI, 115409 Moscow, Russia*

²*Space Physics and Astronomy Research Unit and Sodankylä Geophysical Observatory, University of Oulu, 90014 Oulu, Finland*

³*Institutt for fysikk, NTNU, Trondheim, Norway*

⁴*APC, Université Paris Diderot, CNRS/IN2P3, CEA/IRFU, Observatoire de Paris, Sorbonne Paris Cité, 119 75205 Paris, France*

⁵*Astronomy Department, University of Geneva, Ch. d'Ecogia 16, 1290, Versoix, Switzerland*

⁶*II. Institute for Theoretical Physics, Hamburg University, Hamburg, Germany*

⁷*D.V. Skobeltsyn Institute of Nuclear Physics, Moscow State University, Moscow, Russia and*

⁸*INR RAS, 60th October Anniversary prospect 7a, Moscow, Russia*

(Dated: December 20, 2021)

We compare the predictions of **AAfrag** for the spectra of secondary photons, neutrinos, electrons, and positrons produced in proton-proton collisions to those of the parameterisations of Kamae *et al.*, Kelner *et al.* and Kafexhiu *et al.* We find that the differences in the normalisation of the photon energy spectra reach 20–50% at intermediate values of the transferred energy fraction x , growing up to a factor of two for $x \rightarrow 1$, while the differences in the neutrino spectra are even larger. We argue that LHCf results on the forward production of photons and neutral pions favor the use of the QGSJET-II-04m model on which **AAfrag** is based. The differences in the normalisation have important implications in the context of multi-messenger astronomy, in particular, for the prediction of neutrino fluxes, based on gamma-ray flux measurements, or regarding the inference of the cosmic ray spectrum, based on gamma-ray data. We note also that the positron-electron ratio from hadronic interactions increases with energy towards the cutoff, an effect which is missed using the average electron-positron spectrum from Kelner *et al.* Finally, we describe the publicly available python package **aafragpy**, which provides the secondary spectra of photons, neutrinos, electrons, and positrons. This package complements the **AAfrag** results for protons with energies above 4 GeV with previous analytical parameterisations of particle spectra for lower energy protons.

I. INTRODUCTION

A large variety of applications in astroparticle physics relies on the precise knowledge of the production cross sections of secondary particles in hadronic interactions. A prominent example is the branch of multi-messenger astronomy which aims to connect photon, neutrino and cosmic ray data [1, 2]. While in the past simple estimates or empirical parameterisations for these cross sections were sufficient, the improved accuracy and large statistics of current and future experiments like AMS-02 [3], LHAASO [4], CTA [5] and IceCube-Gen2 [6] requires a corresponding advancement of the theoretical predictions.

There exist two main approaches to the description of hadronic production cross sections. In the first one, one parametrises hadronic interaction data using empirical scaling laws. In spite of its convenience, the use of such parameterisations becomes dangerous when the latter are extrapolated outside the kinematical range of the data, they are based on. In particular, high-energy extrapolations into the multi-PeV range of such empirical parameterizations are generally unreliable, but are required for the correct interpretation of gamma-ray and neutrino data in the 100 TeV–1 PeV energy range. As an alternative, one can use QCD inspired Monte Carlo event generators for the description of hadronic interactions. In order to provide a fast and user-friendly tool for the computation of the production cross sections, one can first bin their results and then either interpolate or

fit them. Given sufficient statistics, the former option reproduces exactly the results of the used Monte Carlo event generator, while the accuracy of the latter approach depends on the choice of appropriate fit functions. Similar to the case of empirical parameterisations, the use of such fit functions becomes dangerous when they are extrapolated outside the fit range.

While most of the QCD inspired Monte Carlo event generators used in cosmic ray physics were overall in a satisfactory agreement [7] with various data from Run I of the Large Hadron Collider (LHC), several of them have been updated by re-tuning their model parameters with LHC data. Moreover, the QGSJET-II-04 model [8, 9] was further tuned in Ref. [10] to improve antiproton production at low energies. The results of this QGSJET-II-04m tune were used to provide **AAfrag** [11, 12] with convenient tabulations of the production cross-sections of secondary particles in proton-proton, proton-nucleus, nucleus-proton, and nucleus-nucleus reactions.

The aim of this work is to compare the predictions of various available parameterisations for the spectra of secondary photons, neutrinos, electrons, and positrons produced in proton-proton collisions to those of **AAfrag**. The predictions of these parameterisations are expected to vary mainly because of differences in the physics of the event generators used to produce the fit data. Moreover, parameterisations based on pre-LHC and post-LHC event generators are expected to differ significantly, especially for forward particle production and in the multi-PeV energy range. In addition, the treatment of the experi-

mental data and the choice of the fit functions affects the predicted spectra. As a result of these differences, we find significant variations between the results of these parametrisations and we characterise the observed discrepancies. In addition, we describe and make publicly available the python package **AAfrag**, which provides the secondary spectra of γ -rays, neutrinos, electrons and positrons for primary proton energies in the energy range $1.5\text{--}10^{11}$ GeV. Since **AAfrag** is restricted to proton energies above 4 GeV, we complement it in this python package at lower energies with the parameterisations of Kamae *et al.* [13].

This article is organised as follows: We start by describing in Section II the main features of the parametrisations we examine. In Section III, we compare secondary particle production for fixed energies of the incident protons, while we discuss the case of an $1/E^2$ primary proton spectrum in Section IV. After a presentation of the new python package **aafrag** in Section V, we conclude.

II. PARAMETRISATIONS

In addition to **AAfrag**, we discuss the three most commonly¹ used parametrisations of Kamae *et al.* [13], Kelner *et al.* [15], and Kafexhiu *et al.* [14]. Their main characteristics are summarized in Table I. A drawback of QCD inspired event generators is that they cannot be used below a minimal energy, which is typically in the range of few to 100 GeV for the energy E_p of the projectile in the lab frame. Note that the recommended minimal energy is with 56 and 100 GeV for Pythia and SIBYLL, respectively, rather high. In contrast, it was shown in Ref. [11] that QGSJET-II-04m can be used down to primary energies as low as 4 GeV. All three parametrisations complement fit functions from event generators at high energies with phenomenological models at low energies. Kamae *et al.* used several parameterized models, including resonance-excitation components for primary energies E_p below 52.6 GeV. Kelner *et al.* proposed to use a δ function approximation for the calculation of the production spectra of secondaries at $E_p \leq 100$ GeV or for $E_s/E_p \leq 10^{-3}$, where E_s denotes the energy of the secondary particle of interest. This approximation is restricted to the case of a power-law spectra in momentum of the proton primaries and the (invalid) assumption of a constant inelastic cross section. Kafexhui *et al.* relied on a compilation of experimental data below $E_p < 2$ GeV and applied GEANT 4.10.0 at intermediate energies. These latter authors considered only the production of photons. Moreover, they re-used the results for the meson spectra from Kelner *et al.* in the case of QGSJET-I and SIBYLL 2.1, but applied different fit functions for the resulting photon spectra. Thus

TABLE I: Characteristics of the models.

	High-energy interaction model	Range in kin. energy, GeV
This work	QGSJET-II-04m	$3.1 - 10^{11}$
Kamae <i>et al.</i>	Pythia 6.2	$0.488 - 5.12 \times 10^5$
Kelner <i>et al.</i>	SIBYLL 2.1	$100 - 10^8$
Kafexhiu <i>et al.</i>	GEANT 4.10.0	$0.280 - 10^5$
	PYTHIA 8.18	$50 - 10^6$
	QGSJET-I	$100 - 10^6$
	SIBYLL 2.1	$100 - 10^6$

one can view the differences between the results of Kafexhui *et al.* and Kelner *et al.* as a measure for the deviations introduced by the fit procedure. Note also that SIBYLL 2.1 was released in the year 2000, while the version of QGSJET-I used in Refs. [14, 15] was published in 1997. Similarly, Pythia 6.2 is a pre-LHC event generator dating from the year 2001.

III. ENERGY SPECTRA FOR MONOENERGETIC PROTONS

A. Photons and neutrinos

We start our comparison with the spectra $E^2 d\sigma/dE$ of photons and neutrinos, produced in proton-proton interactions with fixed primary energies. These spectra, which correspond to the spectral energy distribution (SED) of hypothetical sources of monoenergetic protons, are shown in Figs. 1, 2, and 3. In Fig. 1, which corresponds to the incident proton energy $E_p = 10$ GeV, we observe a 20% scatter in the model results for the photon spectra at the peak of the SED, in the photon energy range $10^{-2}E_p < E_\gamma < 0.1E_p$. The differences between the model predictions grow up to $\sim 50\%$ in the high-energy tails of the SED, which reflects the lack of experimental data for very forward photon production at these energies. The calculated neutrino production spectra shown in the right panel of Fig. 1 deviate somewhat stronger, with $\sim 30\%$ differences. In particular, the SED of **AAfrag** is more sharply peaked in the forward direction than the one of Kamae *et al.*, which reflects the harder spectra of charged pions in QGSJET-II-04m compared to that parametrization.

Moving to higher energies, the differences between **AAfrag** and earlier models stay within 20% at the peak of the SED of secondary particles, cf. with Figs. 2 and 3. On the other hand, the results of the different calculations deviate much stronger in the forward direction, for $x = E_s/E_p \gtrsim 0.1$, where differences exceed 50% for some parametrisations. For the particular case of the model of Kamae *et al.*, this deviation is related to deficiencies in their modelling of inelastic diffraction, as discussed in some detail in Ref. [16]; the corresponding contribu-

¹ For a discussion of other models see Ref. [14]

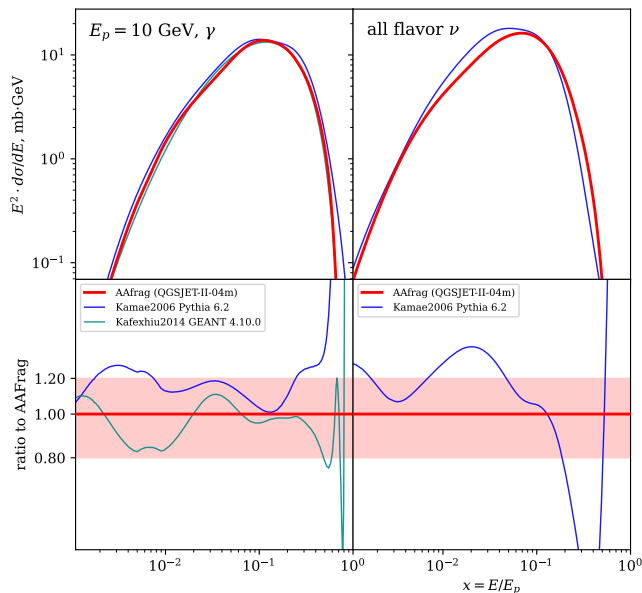


FIG. 1: Gamma-ray (left) and neutrino (right) spectra $E^2 d\sigma/dE$ as a function of the transferred energy fraction $x = E/E_p$, for 10 GeV incident protons. The upper left panel compares the photon spectra calculated with **AAfrag** with those of Kamae *et al.* based on PYTHIA 6.2 and Kafexhiu *et al.* based on GEANT 4.10.0. The spectra of all-flavour neutrinos are compared to Kelner *et al.* and Kamae *et al.* The lower panels show the ratio of the spectra to the **AAfrag** results.

tion is visible by eye as the sharp rise of the blue lines for $E_\gamma \rightarrow E_p$ in the lower left panels of Figs. 2 and 3. On the other hand, the softer photon spectra for $E_\gamma \rightarrow E_p$ obtained in the parametrization of Kafexhiu *et al.*, based on the outdated QGSJET-I model [17], are caused by the too soft pion production spectra in that model. Overall, the increase with energy of the differences between the various predictions for the forward production of secondary particles is due to the fact that relevant experimental data have till recently been available at fixed target energies only, for $E_p \leq 400$ GeV. This lack of experimental data has been especially unsatisfactory, because the role of forward production is greatly enhanced in the case of a steep spectrum of primary cosmic rays, as discussed in some detail in Refs. [16, 18]; this issue will be in this work further addressed in Sec. IV below. Therefore, the measurements of forward photon and neutral pion production at LHC energies, $\sqrt{s} = 0.9, 2.76, 7,$ and 13 TeV, by the LHCf experiment [19–22] are of great importance. In Fig. 4, we compare LHCf measurements (black squares with errorbars) of the differential cross-section of π^0 production at 7 TeV c.m. energy as function of Feynman x_F to the predictions of QGSJET-II-04m (solid red line), SIBYLL 2.1 (dashed-dotted green) and QGSJET-I (dashed blue). It can be seen that QGSJET-II-04m describes overall the data best. The only parametrization which provides enough kinematical information that

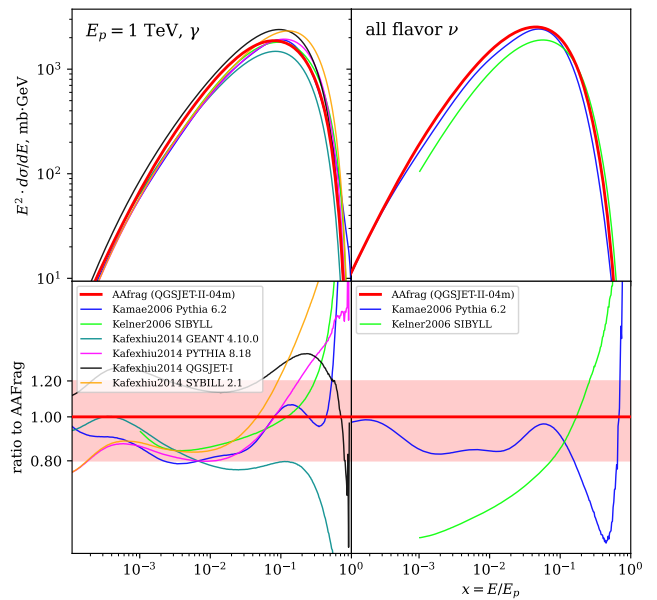


FIG. 2: Gamma-ray and neutrino spectra $E^2 d\sigma/dE$ (top) and ratios (bottom) as a function of the transferred energy fraction $x = E/E_p$, for 1 TeV incident protons. The parametrizations of Kelner *et al.* based on SIBYLL 2.1 and Kafexhiu *et al.* based on SIBYLL, PYTHIA and QGSJET-I are added to the analysis.

it can be compared to such measurements is the one of Kamae *et al.* While 7 TeV c.m. energy is beyond the range of applicability of this parametrization, the predicted yield of photons at 900 GeV c.m. energy is already a factor few above the LHCf measurements. Therefore, the parametrizations of Kamae *et al.* and Kafexhiu *et al.* (blue, green, and magenta lines in Figs. 2 and 3) are disfavored by the LHCf data. Note also that the difference between the results of Kafexhiu *et al.* and Kelner *et al.*, both based on SIBYLL 2.1, which is caused purely by the use of different fit functions, is as large as 20% at $x \simeq 0.1$. Moreover, we observe a rather large discrepancy with the Kelner *et al.* parametrization for the neutrino spectra, where both the normalisation and the shape of the neutrino spectrum differ significantly from the other predictions. As a result, we expect correspondingly large errors in the predictions of the expected number of observable neutrino events from specific sources, which are based on the Kelner *et al.* parametrization.

Figures 1, 2, and 3 also show that the predicted spectral shapes of the photon SED in the limit of small E_γ differ for the various parametrizations. To clarify this point, we plot in Fig. 5 the photon production spectrum $d\sigma/dE$ as function of $\log(E)$ for $E_p = 5$ GeV, calculated using both **AAfrag** and the parametrizations. Plotted in such a way, the photon spectrum should be symmetric with respect to the energy $E_\gamma = m_{\pi^0}/2 \simeq 67.5$ MeV [23]. While this is the case for the Kafexhiu *et al.* results based on GEANT 4.10.0 and for **AAfrag**, this symmetry is broken by the employed fit functions in the case of the

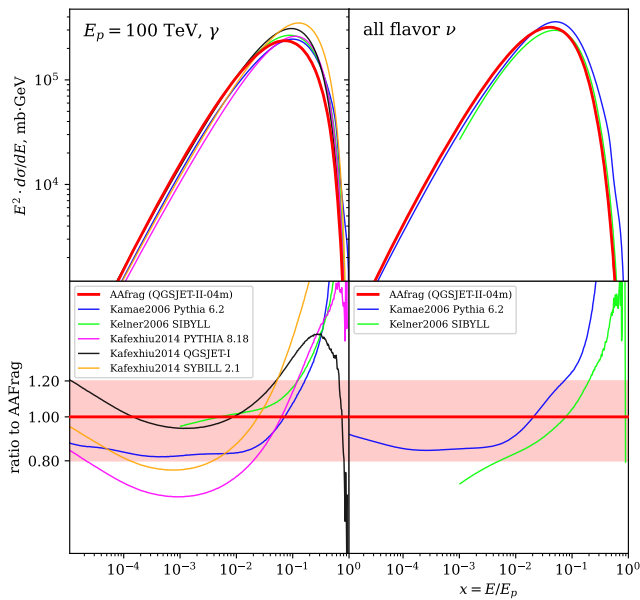


FIG. 3: Same as Fig. 2 for 100 TeV primary protons.

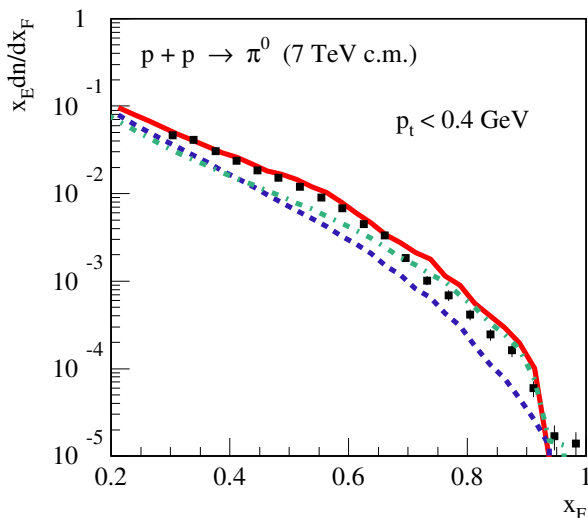


FIG. 4: Measurements of the differential cross-section of π^0 production at 7 TeV c.m. energy as function of Feynman x_F by LHCf (black squares with errorbars) compared to the predictions of QGSJET-II-04m (solid red), SIBYLL 2.1 (dashed-dotted green) and QGSJET-I (dashed blue).

parametrizations. It is worth recalling, however, that the high energy gamma-ray fluxes from astrophysical sources are dominated by the forward photon production in cosmic ray interactions (see, e.g. Ref. [18]). Therefore, the low energy part of the photon production spectra is only relevant to the calculation of photon spectra in the sub-GeV energy range, where the important contributions are coming from proton interactions at relatively low energies.

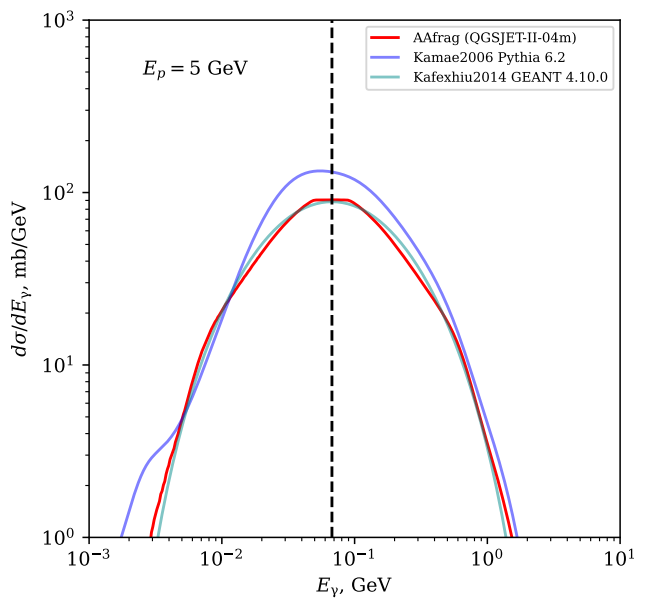


FIG. 5: Differential cross-section of γ -ray production for 5 GeV protons calculated with AAfrag, Kamae *et al.* and Kafexhiu *et al.* codes.

B. Electrons and positrons

In addition to photons and neutrinos, we plot in Fig. 6 the production spectra of positrons and electrons for $E_p = 100$ GeV and 1 TeV, calculated using both AAfrag and the parametrizations. Here, apart from the general differences between the various parametrizations, it is important to note that, unlike AAfrag and Kamae *et al.*, the parametrization of Kelner *et al.* provides average spectra between e^+ and e^- . That way, one neglects the important difference between them, which stems from significantly harder production spectra of π^+ mesons, compared to π^- , in proton-proton interactions. As will be further discussed in Section IV B, this has important consequences for the analysis and the interpretation of experimental data on cosmic-ray fluxes of electrons and positrons.

IV. ENERGY SPECTRA FROM BROAD ENERGY DISTRIBUTIONS OF PROTONS

The intensity I_a of secondary particles of type a is related to the intensity of primary cosmic rays I_p as

$$I_a(E) = \int_0^\infty dl n_{\text{gas}} \int_E^\infty dE' \frac{d\sigma_a(E', E)}{dE} I_p(E'), \quad (1)$$

where the l integration is along a fixed line-of-sight and n_{gas} denotes the number density of target protons. The cosmic-ray spectrum I_p is expected to follow in most of sources roughly a power-law in momentum, modified by

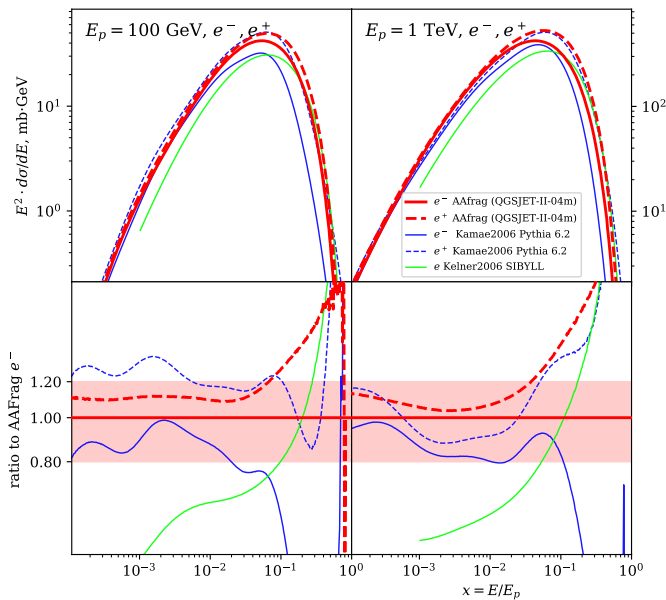


FIG. 6: Electron and positron spectra $E^2 d\sigma/dE$ as a function of the transferred energy fraction $x = E/E_p$, for 100 GeV and 1 TeV incident protons.

a high-energy cutoff which is often chosen as an exponential,

$$I_p(p) = p^{-\gamma} \exp(-p/p_0). \quad (2)$$

In the case of diffusive acceleration on non-relativistic supersonic shocks, one expects $\gamma \simeq 2.0$ – 2.2 [24]. In the following examples, we will use $\gamma = 2$ and use as energy of the cut-off $p_0 = 100$ TeV. Additionally, we will impose a sharp low-energy cut-off at $E_p = 4$ GeV, since the **AAfrag** predictions are available only above this energy.

A. Photon and neutrino spectra

In view of the differences between the predictions of **AAfrag** and of the other parametrizations, for monoenergetic protons, we expect a corresponding spread both for the normalisation and the shapes of the spectra of gamma-rays and neutrinos also for broad energy distributions of primary protons.

In Fig. 7, we compare the spectra of secondary gamma-rays, calculated using **AAfrag**, with the those obtained from the parametrizations. One can see that the overall normalisation of the predicted gamma-ray fluxes varies within $\pm 25\%$ in a wide energy range. In addition, for the parametrizations of Kelner *et al.* and of Kafexhiu *et al.* based on GEANT 4.10.0, we observe a slightly harder energy slope than for **AAfrag**. In the particular case of the parametrization of Kelner *et al.*, this is explained by a too steep energy rise of the inelastic proton-proton cross section, which is at variance with the respective LHC data. On the other hand, the largest differences between

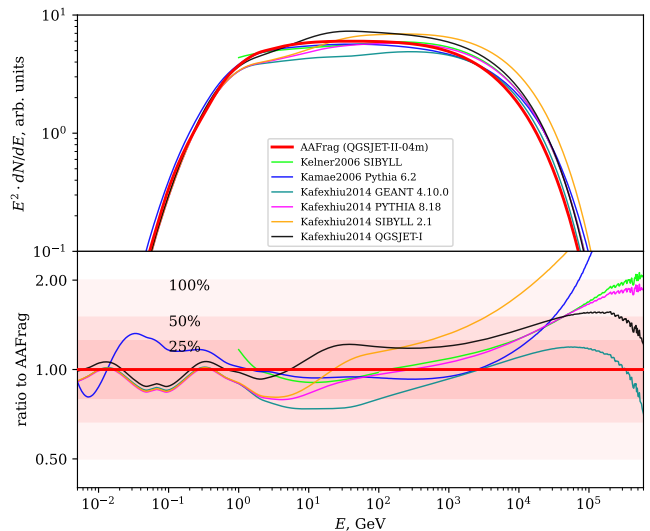


FIG. 7: Gamma-ray energy flux for a power law primary proton spectrum, with an exponential cutoff, $\propto 1/p^2 \exp(-p/p_0)$, $p_0 = 100$ TeV. Upper panel compares the fluxes calculated with **AAfrag** using QGSJET-II-04m and the ones of [15] based on SIBYLL, [13] based on PYTHIA 6.2, and [14] based on GEANT 4.10.0, PYTHIA 8.18, and QGSJET-I. Lower panel shows the ratio of the fluxes for the different parametrizations to the one of **AAfrag**.

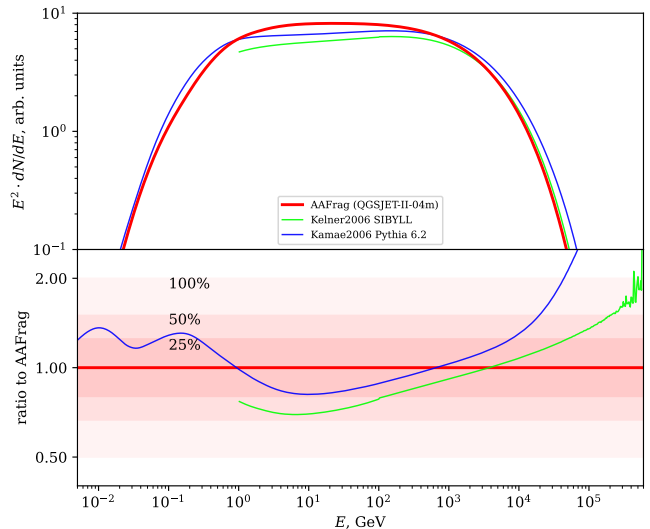


FIG. 8: All flavor neutrino flux for a power-law cosmic ray spectrum ($\propto 1/p^2 \exp(-p/p_0)$).

the various predictions concern the spectral shape in the vicinity of the high-energy cut-off, where the spread reaches a factor of two. This is not surprising since the steep fall-down of the primary proton spectrum in the cutoff region greatly enhances the sensitivity of the results to very forward ($E_\gamma \rightarrow E_p$) photon production in proton-proton interactions, for which substantial differences between the model predictions have been observed

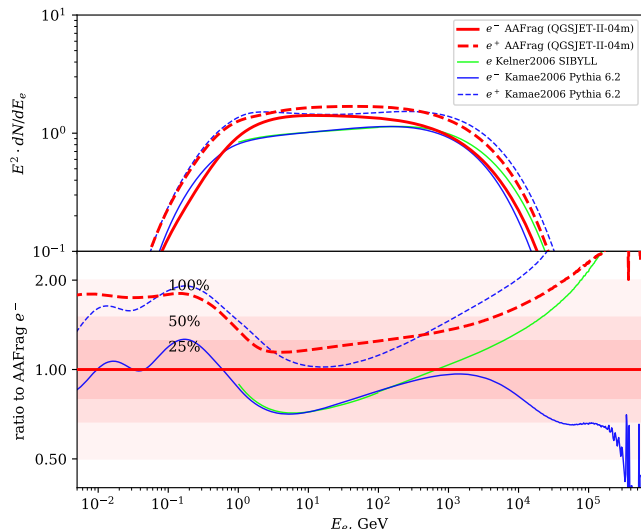


FIG. 9: Electron and positron fluxes for a power-law cosmic ray spectrum ($\propto 1/p^2 \exp(-p/p_0)$).

in the previous section (c.f. Figs. 2 and 3). While the harder gamma-ray fluxes predicted by Kamae *et al.* is caused by deficiencies in the modeling of the diffractive scattering, the harder slope of the pion spectrum predicted by SIBYLL 2.1 results in a corresponding rise of the photon spectrum in the parametrisations of Kelner *et al.* and Kafexhiu *et al.*. This may have important consequences for the modelling of the new population of PeV gamma-ray sources recently discovered by Tibet-AS γ [25] and LHAASO [26].

In Fig. 8, we show the comparison of the all-flavor neutrino spectra obtained with **AAfrag** and the different parametrizations. Here, **AAfrag** differs from the other models even stronger. In particular, **AAfrag** predicts an up to 50% higher flux of neutrinos, over a broad energy range except the cutoff region, compared to the model of Kelner *et al.* The agreement with Kamae *et al.* is better, with differences within 25%. However, the high-energy cut-off in the neutrino spectra of Kamae *et al.* is much sharper. This implies that the model predictions for neutrino events might differ by up to a factor of two.

B. Electron and positron spectra

In the upper panel of Fig. 9, we show the electron and positron fluxes produced by the modelled power-law cosmic-ray spectrum and calculated with **AAfrag** and Kamae *et al.*, together with the average electron-positron spectrum from Kelner *et al.* The lower panel shows the ratio of these spectra to the electron spectrum calculated with **AAfrag**. We note first that both the normalisation and the shape of the positron and electron spectra differ. While in **AAfrag** there are $\simeq 20\%$ more positrons than electrons at few GeV, this surplus exceeds a factor

two close to the cutoff. As a result, the positron-electron ratio from hadronic interactions increases with energy towards the cutoff, an effect which is missed using the average electron-positron spectrum from Kelner *et al.*

V. AAFRAGPY PYTHON PACKAGE

So far we explored differences between the results of the various parameterisations, imposing a sharp low-energy cut-off at the primary particle energy $E_p = 4$ GeV, given that the energy range of **AAfrag** is constrained to $E_p > 4$ GeV. Realistic astrophysical source spectra generally extend to lower energies and **AAfrag** cannot be directly used in such settings.

To overcome this limitation, we have developed a Python package that implements a Python interface to **AAfrag** and allows to complement **AAfrag** based calculations of particle production spectra with calculations based on parameterisations of low energy production cross-sections. The package can be installed through the standard *pip* installer (`pip install aafragpy`). It provides several functions:

- The matrix of differential cross-sections of secondary particle production in nuclear interaction for a given combination of primary and target nuclei for a given range of energies (function `get_cross_section`);
- The differential spectrum of secondary particles produced in the interaction of a given primary spectrum with target nuclei (function `get_spectrum`).

We have included two alternative parameterisations of production cross-sections: those of Kamae *et al.* [13] and of Kafexhiu *et al.* [14]. The functions for the calculation of differential cross-sections and spectra for these parameterisations are supplemented by `_Kamae2006` and `_Kafexhiu2014` suffixes. Both parameterisations can be used only for the calculation of *pp* cross-sections.

Figure 10 shows an example of calculation of the spectrum of γ -rays from proton-proton interactions, for a power-law proton spectrum with exponential cutoff using such a combined approach. The **AAfrag** production spectrum calculated for protons with energies $E_p > 4$ GeV is shown by the red solid line. The spectrum is complemented by the spectrum of γ -rays produced by protons with energies $E \leq 4$ GeV, calculated using the Kamae *et al.* [13] parameterisation, shown by the blue dotted line. The sum of the two spectra, shown by the blue solid line, corresponds to the total γ -ray spectrum from a proton distribution in a broad energy range.

VI. CONCLUSIONS

We have compared the predictions of **AAfrag** for the spectra of secondaries produced in proton-proton collisions to those of three often used parameterisations. We

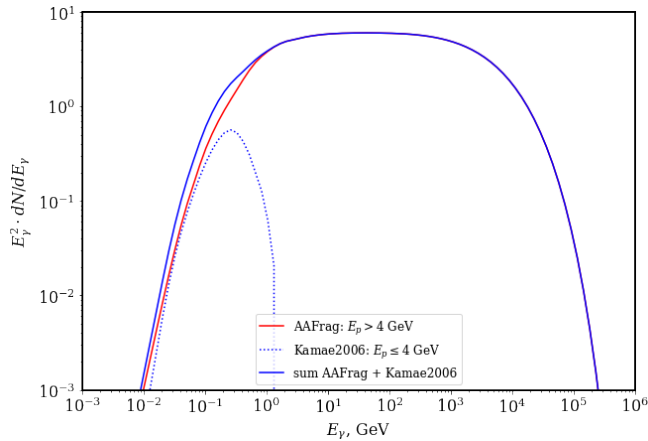


FIG. 10: Example of the spectrum of γ -ray emission from pp interactions for an $dN/dp \propto p^{-2}$ powerlaw proton with cutoff on $p_0=100$ TeV. The spectrum generated by **AAfrag** for proton energies > 4 GeV is complemented by the spectrum calculated using the parameterisations of Kamae et al. [13] for $E_p < 4$ GeV. An url to interactive Python notebook for the calculation of this spectrum can be found at GitHub page of the project: <https://github.com/aafraqpy/aafraqpy>

have found considerable differences both in the normalisation and the shape of the energy spectra, especially in the region of large energy transfer. A part of these variations is caused by the (unnecessary) procedure of fitting the results of QCD based event generators. More importantly, several parametrisations are based on outdated pre-LHC event generators. In the case of the energy

spectra of photons, we have argued that LHCf results on the forward production of photons favor the use of the QGSJET-II-04 model on which **AAfrag** is based on. We have also stressed that the use of the average electron-positron spectrum misses the increase with energy of the positron-electron ratio in hadronic interactions.

The differences found in the normalisation of the secondary spectra have important implications in the context of multi-messenger astronomy, in particular, for the prediction of neutrino fluxes based on gamma-ray flux measurements, or regarding the inference of the cosmic ray spectrum based on gamma-ray data.

We also present the easy-to-use Python package **aafraqpy**, which allows calculating the differential cross-section and the spectrum of secondary particles produced in nucleus-nucleus interactions in the astrophysical sources. The package uses the calculations of the original **AAfrag** together with calculations performed by Kamae et al. [13] and Kafexhiu et al. [14] for low-energy secondary production.

Acknowledgments

S.O. acknowledges support from the Deutsche Forschungsgemeinschaft (project number 465275045). S.K. acknowledges support from the Ministry of Science and Higher Education of the Russian Federation under project “Fundamental problems of cosmic rays and dark matter” No. 0723-2020-0040.

-
- [1] M. Spurio, *Probes of Multimessenger Astrophysics*, Astron. Astrophys. Lib. (Springer, 2018).
 - [2] M. Kachelrieß and D. V. Semikoz, Prog. Part. Nucl. Phys. **109**, 103710 (2019), 1904.08160.
 - [3] M. Aguilar et al. (AMS), Phys. Rept. **894**, 1 (2021).
 - [4] X. Bai et al. (2019), 1905.02773.
 - [5] B. S. Acharya et al. (CTA Consortium), *Science with the Cherenkov Telescope Array* (WSP, 2018), ISBN 978-981-327-008-4, 1709.07997.
 - [6] M. G. Aartsen et al. (IceCube-Gen2), J. Phys. G **48**, 060501 (2021), 2008.04323.
 - [7] D. d’Enterria, R. Engel, T. Pierog, S. Ostapchenko, and K. Werner, Astropart. Phys. **35**, 98 (2011), 1101.5596.
 - [8] S. Ostapchenko, Phys. Rev. **D83**, 014018 (2011), 1010.1869.
 - [9] S. Ostapchenko, EPJ Web Conf. **52**, 02001 (2013).
 - [10] M. Kachelrieß, I. V. Moskalenko, and S. S. Ostapchenko, Astrophys. J. **803**, 54 (2015), 1502.04158.
 - [11] M. Kachelrieß, I. V. Moskalenko, and S. Ostapchenko, Comput. Phys. Commun. **245**, 106846 (2019), 1904.05129.
 - [12] *AAfrag: interpolation routines for secondary production*, available at <https://sourceforge.net/projects/aafraq/>.
 - [13] T. Kamae, N. Karlsson, T. Mizuno, T. Abe, and T. Koi, Astrophys. J. **647**, 692 (2006), [Erratum: Astrophys. J. **662**, 779 (2007)], astro-ph/0605581.
 - [14] E. Kafexhiu, F. Aharonian, A. M. Taylor, and G. S. Vila, Phys. Rev. D **90**, 123014 (2014), 1406.7369.
 - [15] S. R. Kelner, F. A. Aharonian, and V. V. Bugayov, Phys. Rev. D **74**, 034018 (2006), [Erratum: Phys.Rev.D **79**, 039901(E) (2009)], astro-ph/0606058.
 - [16] M. Kachelrieß and S. Ostapchenko, Phys. Rev. **D86**, 043004 (2012), 1206.4705.
 - [17] N. N. Kalmykov and S. S. Ostapchenko, Phys. Atom. Nucl. **56**, 346 (1993).
 - [18] M. Kachelrieß, I. V. Moskalenko, and S. S. Ostapchenko, Astrophys. J. **789**, 136 (2014), 1406.0035.
 - [19] O. Adriani et al. (LHCf), Phys. Lett. **B703**, 128 (2011), 1104.5294.
 - [20] O. Adriani et al. (LHCf), Phys. Lett. **B715**, 298 (2012), 1207.7183.
 - [21] O. Adriani et al. (LHCf), Phys. Rev. **D94**, 032007 (2016), 1507.08764.
 - [22] O. Adriani et al. (LHCf), Phys. Lett. **B780**, 233 (2018), 1703.07678.
 - [23] F. Stecker, *Cosmic Gamma Rays* (Mono Book Corporation, Baltimore, 1971).

- [24] A. R. Bell, *Astropart. Phys.* **43**, 56 (2013).
- [25] M. Amenomori et al. (Tibet ASgamma), *Phys. Rev. Lett.* **126**, 141101 (2021), 2104.05181.
- [26] Z. Cao, F. A. Aharonian, Q. An, Axikegu, L. X. Bai, Y. X. Bai, Y. W. Bao, D. Bastieri, X. J. Bi, Y. J. Bi, et al., *Nature* **594**, 33 (2021), ISSN 14764687.